

# Kinetics of consumption of fermentation products by anode-respiring bacteria

César I. Torres · Andrew Kato Marcus ·  
Bruce E. Rittmann

Received: 4 June 2007 / Revised: 18 August 2007 / Accepted: 6 September 2007  
© Springer-Verlag 2007

**Abstract** We determined the kinetic response of a community of anode-respiring bacteria oxidizing a mixture of the most common fermentation products: acetate, butyrate, propionate, ethanol, and hydrogen. We acclimated the community by performing three consecutive batch experiments in a microbial electrolytic cell (MEC) containing a mixture of the fermentation products. During the consecutive-batch experiments, the coulombic efficiency and start-up period improved with each step. We used the acclimated biofilm to start continuous experiments in an MEC, in which we controlled the anode potential using a potentiostat. During the continuous experiments, we tested each individual substrate at a range of anode potentials and substrate concentrations. Our results show low current densities for butyrate and hydrogen, but high current densities for propionate, acetate, and ethanol (maximum values are 1.6, 9.0, and 8.2 A/m<sup>2</sup>, respectively). Acetate showed a high coulombic efficiency (86%) compared to ethanol and propionate (49 and 41%, respectively). High methane concentrations inside the MEC during ethanol experiments suggest that methanogenesis is one reason why the coulombic efficiency was lower than that of acetate. Our results provide kinetic parameters, such as the anode overpotential, the maximum current density, and the Monod half-saturation constant, that are needed for model

development when using a mixture of fermentation products. When we provided no electron donor, we measured current due to endogenous decay of biomass (~0.07 A/m<sup>2</sup>) and an open-cell potential (-0.54 V vs Ag/AgCl) associated with biomass components active in endogenous respiration.

**Keywords** Coulombic efficiency · Fermentation products · Microbial electrolytic cell · Open-cell potential

## Introduction

Anode-respiring bacteria (ARB) are able to transfer electrons to a solid conductive anode as part of their energy-generating respiration. ARB are of special interest for generating electrical current directly from the electrons contained in biodegradable organic compounds present in wastes and other forms of biomass. The energy in the electrons can be harvested as electrical power in a microbial fuel cell (MFC) or as hydrogen (H<sub>2</sub>) in a microbial electrolytic cell (MEC; Liu et al. 2005a). Electricity generation using MFCs has been studied using simple organic compounds, such as acetate, butyrate, and glucose (Chaudhuri and Lovley 2003; Min and Logan 2004; Liu et al. 2005b); complex organic matter, such as wastewater sludge and swine wastes (Dentel et al. 2004; Min et al. 2005); and inorganic electron donors, such as sulfide (Rabaey et al. 2006). Thus, ARB can have the dual benefit of harvesting energy and removing pollutants from water.

Fermentation appears to be an important process in an MFC (or MEC) utilizing complex organic substrates. Fermentative bacteria can hydrolyze and ferment complex organic substrates to simple organic acids (e.g., propionate,

---

**Electronic supplementary material** The online version of this article (doi:10.1007/s00253-007-1198-z) contains supplementary material, which is available to authorized users.

---

C. I. Torres (✉) · A. Kato Marcus · B. E. Rittmann  
Center for Environmental Biotechnology, Biodesign Institute at  
Arizona State University,  
Tempe, AZ 85287-5701, USA  
e-mail: cit@asu.edu

butyrate, and acetate) and/or alcohols (e.g., ethanol), which ARB can utilize. Fermentation and anode-respiration processes can be combined in two different ways. Hydrolysis and fermentation can occur in the same reactor with the ARB, creating a mixture of fermentative bacteria and ARB at the biofilm anode surface. Alternatively, hydrolysis and fermentation can be separated into an independent reactor, and the MFC/MEC receives simpler organic compounds typical of fermentation effluent, which should be able to be consumed directly by ARB. Although it is not obvious a priori which scenario is better for achieving higher energy-conversion efficiencies, separating the processes simplifies the goal of our study, which is to determine the function of an ARB community.

The effectiveness of ARB to consume different fermentation products will influence how the fermentation pretreatment is optimized. A change in pH can affect the fermentation pathway used by bacteria, thus altering the composition of fermentation products (Yu and Fang 2003; Ying and Yang 2004; Hwang et al. 2004). Some fermentation pathways, such as the acetate/butyrate type (Wu and Lin 2004) and the ethanol/acetate type (Ren et al. 1997), also have the advantage of producing significant amounts of biohydrogen as a useful energy carrier. Thus, the dual-treatment process of fermentation and MFC/MEC should be carefully optimized to obtain the maximum benefit in the form of H<sub>2</sub> and/or electrical energy.

The objectives of our study were to assess the relative ability of ARB to generate electricity continuously from a mixture of the most common fermentation products, simulating a real fermentation effluent in which various substrates are present together, and to estimate important parameters that represent the kinetics for their consumption. We performed continuous experiments using an enriched ARB community grown with a mixture of the fermentation products of interest. We analyzed how the kinetics of consumption of the individual substrate were affected by the anode potential and substrate concentration. Our results provide necessary kinetic parameters for modeling MFC/MEC operation using a fermentation products mixture.

## Thermodynamic and kinetic background

Our experiments study the capability of a mixed ARB community to consume simple fermentation products: acetate, butyrate, propionate, ethanol, and H<sub>2</sub>. Table 1 shows the reduction half reactions of the most common fermentation products and their thermodynamic potentials. As substrate oxidation proceeds and current is produced, the extracted electrons lose energy, and thus, the electrons' potential becomes higher than the potential shown in Table 1. Thus, the working potential at the anode must also be higher than the substrate potential. The energy loss from the open-cell potential (OCP) to the potential needed to achieve a certain current density is defined as overpotential (Rabaey and Verstraete 2005).

The anode potential ( $V_{\text{anode}}$ ) controls the kinetics of electron transfer from ARB to the anode. The mathematical expressions that describe the relationship between the rate of current production and the anode potential are based on two distinct mechanisms. Zhang and Halme (1995) and Picioreanu et al. (2007) consider the electron-shuttle mechanisms, in which the transfer of electrons between bacteria and the anode surface is mediated by soluble electron mediators. In contrast, Kato-Marcus et al. (2007) consider the conduction of electrons through the biofilm matrix that carries electrons from bacteria to the anode surface. Although these models describe electron transfer from the bacteria to the anode using distinctly different mechanisms, the models agree that current generation increases with increasing anode potential until a saturation value is reached.

The rate of substrate utilization in microbial processes is frequently modeled using the Monod relationship (Rittmann and McCarty 2001). When the aqueous substrate is the only rate-limiting substrate, the rate of substrate utilization can be written as Eq. 1 for the biofilm setting:

$$r_{\text{ut}} = q_{\text{max}} X_{\text{f}} L_{\text{f}} \frac{S}{K_{\text{s,app}} + S} \quad (1)$$

**Table 1** Reduction half reactions and reaction potentials for the common fermentation products studied

Substrate	Half reaction	$E^{\circ}$ (V vs Ag/AgCl)	$E$ (V vs Ag/AgCl)
Acetate	$1/8\text{CO}_2 + 1/8\text{HCO}_3^- + \text{H}^+ + e^- \rightarrow 1/8\text{CH}_3\text{COO}^- + 3/8\text{H}_2\text{O}$	-0.481	-0.505
Butyrate	$1/20\text{HCO}_3^- + 3/20\text{CO}_2 + \text{H}^+ + e^- \rightarrow 1/20\text{CH}_3\text{CH}_2\text{CH}_2\text{COO}^- + 7/20\text{H}_2\text{O}$	-0.484	-0.514
Propionate	$1/7\text{CO}_2 + 1/14\text{HCO}_3^- + \text{H}^+ + e^- \rightarrow 1/14\text{CH}_3\text{CH}_2\text{COO}^- + 5/14\text{H}_2\text{O}$	-0.483	-0.511
Ethanol	$1/6\text{CO}_2 + \text{H}^+ + e^- \rightarrow 1/12\text{CH}_3\text{CH}_2\text{OH} + 1/4\text{H}_2\text{O}$	-0.521	-0.544
H <sub>2</sub>	$\text{H}^+ + e^- \rightarrow 1/2\text{H}_2$	-0.611	-0.605

For the third column, standard reaction potentials are for pH=7 and  $T=25^{\circ}\text{C}$ . For the last column, reaction potentials are for typical experimental conditions:  $T=30^{\circ}\text{C}$ ,  $[\text{Substrate}] = 20e^{-}\text{meq}/1$ ,  $[\text{CO}_2] = [\text{HCO}_3^-] = 5\text{mM}$ , and pH=7.4. For H<sub>2</sub>,  $P_{\text{H}_2} = 0.1\text{ atm}$ .

where  $r_{\text{ut}}$  is the rate of substrate utilization per surface area ( $M_s L^{-2} T^{-1}$ ),  $q_{\text{max}}$  is the maximum specific rate of substrate utilization ( $M_s M_x^{-1} T^{-1}$ ),  $X_f$  is the concentration of active biomass in the biofilm ( $M_x L^{-3}$ ),  $L_f$  is the biofilm thickness ( $L$ ),  $K_{s, \text{app}}$  is the apparent half saturation substrate concentration in a biofilm ( $M_s L^{-3}$ ), and  $S$  is the substrate concentration in the liquid ( $M_s L^{-3}$ ).

Substrate utilization is divided into substrate oxidized for energy generation (respiration) and substrate used by bacteria for cell synthesis. As part of biomass decay, some of the biomass is oxidized in endogenous respiration. Therefore, the current generated by ARB is the sum of the respiration rates associated with substrate utilization and biomass decay:

$$j = \gamma_s q_{\text{max}} X_f L_f \frac{S}{K_{s, \text{app}} + S} (1 - f_s^0) + \gamma_x b X_f L_f \quad (2)$$

where  $j$  is the current density obtained by ARB ( $IL^{-2}$ ),  $\gamma_s$  and  $\gamma_x$  are conversion factors from mass to coulombs for the substrate and biomass ( $[e^- \text{ eq} \times F]/MW$ ),  $f_s^0$  is the fraction of electrons used for cell synthesis, and  $b$  is the endogenous-decay coefficient ( $T^{-1}$ ).  $j_{\text{max}}$  is the maximum current achievable and is defined by:

$$j_{\text{max}} = \gamma_s q_{\text{max}} X_f L_f (1 - f_s^0) + \gamma_x b X_f L_f \quad (3)$$

In an ideal case of a pure-ARB biofilm, the coulombic efficiency obtained, assuming complete depletion of the substrate, is equal to the ratio of the current generated to the total rate of substrate utilization:

$$\text{Ideal Coulombic Efficiency} = \frac{j}{\gamma_s r_{\text{ut}}} = (1 - f_s^0) + \frac{\gamma_x b X_f L_f}{\gamma_s r_{\text{ut}}} \quad (4)$$

However, the presence of  $e^-$  sinks other than the anode (e.g., methane, hydrogen, unoxidized fermentation products, and non-ARB biomass) will cause this coulombic efficiency to decrease from its ideal value.

## Materials and methods

### Reactor and medium components

We used two dual-compartment H-type MECs: one for batch acclimation experiments and one for continuous experiments. The MECs held 300 ml in each compartment, and the compartments were separated by a cation exchange membrane (CMI 7000, Membranes International). Each cathode compartment contained a 0.79-cm OD graphite rod ([www.graphitestore.com](http://www.graphitestore.com)) as an electrode for  $H_2$  production, with a total surface area of 20.5  $cm^2$ . The batch MEC anode

compartment contained three similar graphite rods, for a total surface area of 61.5  $cm^2$ . The continuous MEC anode compartment contained a carbon felt (Alfa Aesar, Massachusetts, USA) with a total geometrical surface area of 93.5  $cm^2$  ( $7.6 \times 5.6 \times 0.318$  cm). We placed an Ag/AgCl reference electrode in each anode compartment (BASI Electrochemistry, MF-2052) less than 1 cm apart from the working electrode to control the anode potential using a potentiostat. We assumed that Ag/AgCl is +0.197 V with respect to SHE for all thermodynamic calculations (Bard and Faulkner 2001). Before starting the experiment, we sparged each compartment with  $N_2$  to remove oxygen and sealed it gas-tight; we then wrapped the entire MEC in aluminum foil to shield it from light. The use of an MEC ( $H_2$  production in the cathode) allowed us to minimize the possibility of oxygen diffusion into the biofilm caused by the use of  $O_2$  as electron acceptor in an MFC setup, which can affect the growth of ARB and reduce coulombic efficiency. We continued to sparge  $N_2$  at 60 ml/min in each cathode compartment to minimize  $H_2$  diffusion from the cathode compartment to the anode compartment. Each MEC compartment was agitated at 150 rpm with a magnetic stir bar and maintained at 30°C.

The anode and cathode compartments contained medium having these common components in 1 l of reverse-osmosis water: 2.85 g NaCl, 1.69 g  $KH_2PO_4$ , and 12.4 g  $Na_2HPO_4$ . The anode compartment also contained 0.038 g  $NH_4Cl$  and a mineral solution with the following final concentrations (in g/l): 5 mg EDTA, 30 mg  $MgSO_4 \cdot 7H_2O$ , 5 mg  $MnSO_4 \cdot H_2O$ , 10 mg NaCl, 1 mg  $FeSO_4 \cdot 7H_2O$ , 1 mg  $Co(NO_3)_2 \cdot H_2O$ , 1 mg  $CaCl_2$ , 1 mg  $ZnSO_4 \cdot 7H_2O$ , 0.1 mg  $CuSO_4 \cdot 5H_2O$ , 0.1 mg AlK ( $SO_4$ )<sub>2</sub>, 0.1 mg  $H_3BO_3$ , 0.1 mg  $Na_2MoO_4 \cdot 2H_2O$ , 0.01 mg  $Na_2SeO_3$ , 0.1 mg  $Na_2WO_4 \cdot 2H_2O$ , and 0.2 mg  $NiCl_2 \cdot 6H_2O$ . The substrate concentrations (added as sodium acetate, propionic acid, butyric acid, and/or anhydrous ethanol) varied with the experiments and are noted below. For the  $H_2$  experiments, we sparged 10%  $H_2$ /Bal  $N_2$  directly to the anode compartment using the nutrient medium described above with no other substrate added.

We acclimated an ARB community by performing a three-step batch acclimation in an MEC that contained a mixture of the fermentation products studied (except  $H_2$ ). We seeded the first batch step with 3 ml of return activated sludge return from Mesa Northwest Water Reclamation Plant (Mesa, AZ, USA). We grew a biofilm capable of generating current from the fermentation products for at least 6 days. Then, we used the biofilm grown on the electrode surface as inoculum for the next batch step. We repeated this procedure three times to select ARB within the original seed. We used the biofilm contained in one electrode (20.5  $cm^2$ ) from the third batch step as inoculum for the continuous MEC used in this study.

We operated the continuous MEC reactor in batch mode with a substrate mixture (40  $e^-$  meq/l of acetate, butyrate, and propionate; 60  $e^-$  meq/l of ethanol) for 5 days, when it reached a total current of  $\sim 5$  mA. After this, we began continuous flow and varied the influent flow rate to find a suitable hydraulic retention time (HRT) for the experiments (data on variations not shown). The HRT was 5.7 h for all experiments for which we present results. After the MEC gave a stable current density with an HRT of 5.7 h, we changed the influent feed to contain only one substrate at a concentration of 100  $e^-$  meq/l and pH in the range 7.4–7.5. We fed each substrate for at least 24 h, and the MEC reached a steady-state current before we performed short-term experiments by varying anode potential or substrate concentration.

#### Potential control

We controlled the anode potential with a potentiostat (Princeton Applied Research, Model 363, Tennessee, USA) at +0.1 V vs Ag/AgCl for all experiments except for short-term current density–voltage ( $j$ –V) experiments. The potentiostat is a powerful electrochemical tool for studying the processes occurring at the working electrode (the anode in this case) in isolation from the other processes occurring in the cell (Wang 2000); a potentiostat provides energy to an MFC/MEC to compensate for the voltage drop caused by the cathode overpotential and ohmic resistance, thereby allowing a fixed anode potential that does not depend on reactions at the cathode. Therefore, current density is only limited by the anode processes, which are the focus of our research. Previous researchers used potentiostats to grow ARB communities at a constant anode potential (Bond and Lovley 2003; Chaudhuri and Lovley 2003). During our experiments, the potential provided by the potentiostat between the anode and the cathode was 4 to 6 V. We collected data in intervals of 2 min using LABVIEW and a National Instruments BNC-2110 analog interface. We carried out short-term  $j$ –V experiments by waiting at least 45 min at each condition and averaging the last 20 min of data. We normalized the reported current to the geometrical electrode surface area for comparison among experiments and computed the coulombic efficiency as the ratio of electrons recovered through the external circuit to the electron equivalence of substrate(s) consumed; Table 1 shows the stoichiometry.

#### Chemical analytical procedures

We analyzed effluent samples for ethanol, acetate, butyrate, and propionate concentrations using high-performance liquid chromatography (Shimadzu LC-

20AT, Japan) with an Aminex HPX-87H column (Biorad Laboratories, Milan, Italy) at 30°C and with diode array and refractive index detectors. The eluent was 2.5 mM H<sub>2</sub>SO<sub>4</sub> at 0.6 ml/min. We measured concentrations of H<sub>2</sub> and methane in the headspace of the reactors using a gas chromatograph (Shimadzu GC-2010, Japan) with a packed column (Restek 19808, Pennsylvania, USA) at 140°C using N<sub>2</sub> at 10 ml/min as carrier gas and a thermal conductivity detector.

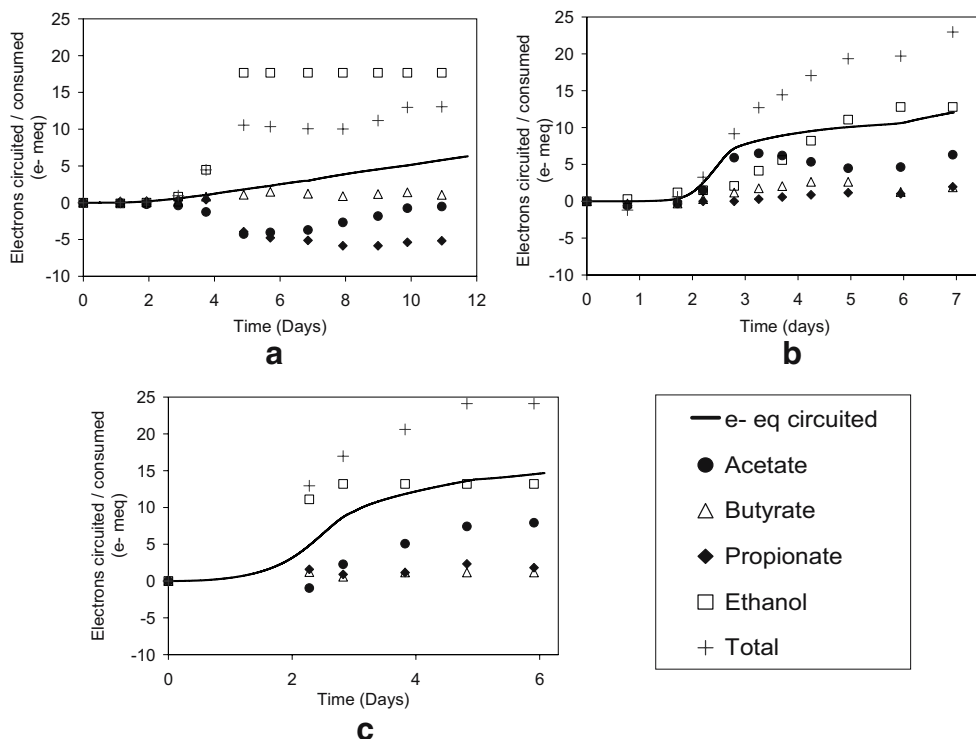
## Results

### Batch experiments

To study the simultaneous oxidation of fermentation products by ARB, we performed batch experiments containing a mixture of fermentation products. Figure 1 shows the results for three consecutive batch experiments. The initial concentrations were 40  $e^-$  meq/l each for acetate, propionate, and butyrate for all experiments, 60  $e^-$  meq/l of ethanol for the first batch experiment, and 44  $e^-$  meq/l of ethanol for the second and third batch experiments. The graphs track the consumption of the individual substrates over time, as well as the electron equivalents circuited (calculated from the total current). We inoculated the first batch experiment as described in the “[Materials and methods](#).” The second and third batch experiments were inoculated by scraping the biofilm off of one anode electrode (20.5 cm<sup>2</sup>) from the previous batch experiment. The result of this acclimation is shown by higher current densities, higher coulombic efficiencies, and smaller lag periods compared to the previous batch experiment.

The first batch experiment shows a fast consumption of ethanol, probably due to fermentation, as acetate and propionate were produced (shown as a negative consumption). Subsequently, most of the acetate produced was consumed, along with some propionate and butyrate. The second and third experiments also show some fermentation effects, with the production of acetate and propionate (and butyrate in the second experiment) from ethanol. In these experiments, acetate and ethanol were consumed at a faster rate, compared to the consumption of propionate and butyrate. The final coulombic efficiencies for the first, second, and third experiments were 45, 52, and 60%, respectively, based on the current generated over the total substrate consumed. The increased coulombic efficiency suggests that ARB were selectively accumulated in comparison to bacteria capable of consuming the substrates by alternate pathways (e.g., methanogenesis and fermentation to products that ARB cannot utilize).

**Fig. 1** Electron equivalents consumed (for each individual substrate) or circuited in three consecutive (a, b, c) batch-reactor experiments. Negative values indicate production of the specific substrate. “Total” refers to the sum of all the substrate concentrations. The inoculum for the next batch experiment was the attached biofilm from the previous experiment



Continuous experiments

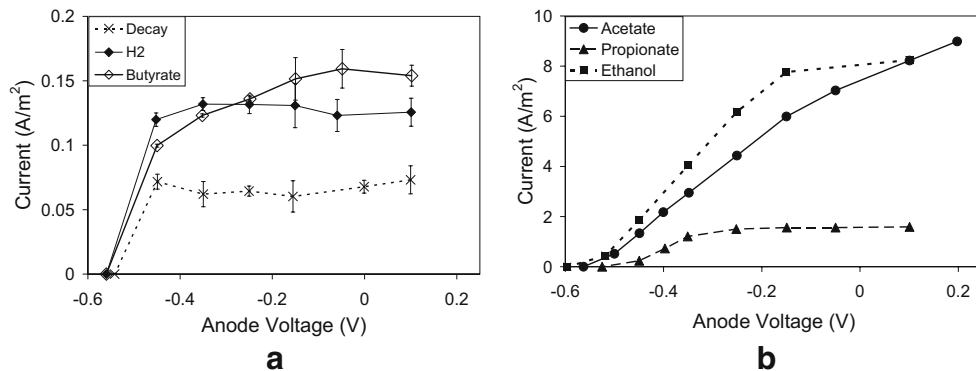
Figure 2 shows how the current density responded to anode potential in the continuous MEC for the following: no substrate, acetate, propionate, butyrate, ethanol, or H<sub>2</sub>. We performed the no-substrate *j*-*V* experiment by flushing the system with nutrient medium containing no electron donor or organic-carbon source. Given no exogenous electron sources, current generated came solely from biomass self-oxidation, or endogenous decay. The current density due to decay ( $\gamma_x b X_f L_f \sim 0.07$  A/m<sup>2</sup>, Fig. 2a) was two orders of magnitude smaller than the maximum current density we achieved ( $\sim 9$  A/m<sup>2</sup>, Fig. 2b).

The continuous MEC was not able to consume H<sub>2</sub> rapidly (Fig. 2a), showing a current only slightly higher than the decay current (0.16 A/m<sup>2</sup>, Fig. 2a). This is consistent with our previous experiments, explained in the Supplementary Material S1, where we compare the current

output of MFCs fed with H<sub>2</sub> or a combination of acetate and H<sub>2</sub>. The continuous MEC experiment also showed a small current density for butyrate (0.16 A/m<sup>2</sup>, Fig. 2a). We did not perform additional kinetic studies for butyrate and H<sub>2</sub> due to the low current density obtained.

The *j*-*V* curves in Fig. 2b demonstrate that acetate, ethanol, and propionate were consumed more effectively in the continuous MEC than H<sub>2</sub> and butyrate. The maximum current density for ethanol was 8.24±0.05 A/m<sup>2</sup>, and it started to saturate at -0.15 V. Ethanol showed the smallest overpotential of the substrates studied, shown by its *j*-*V* curve having a sharper increase in current density with anode potential. Acetate had a maximum current density of 8.98±0.08 A/m<sup>2</sup>, but it did not saturate within the range of anode potentials studied, creating a higher overpotential and, thus, a higher energy loss. The propionate current density was lower (maximum of 1.58±0.01 A/m<sup>2</sup>) than for acetate and ethanol, but still

**Fig. 2** *j*-*V* curves for various individual substrates typical of a fermentation effluent. Voltage values were measured vs Ag/AgCl. Note the different scales on the vertical axes. a Decay, H<sub>2</sub>, and butyrate. b Acetate, propionate, and ethanol



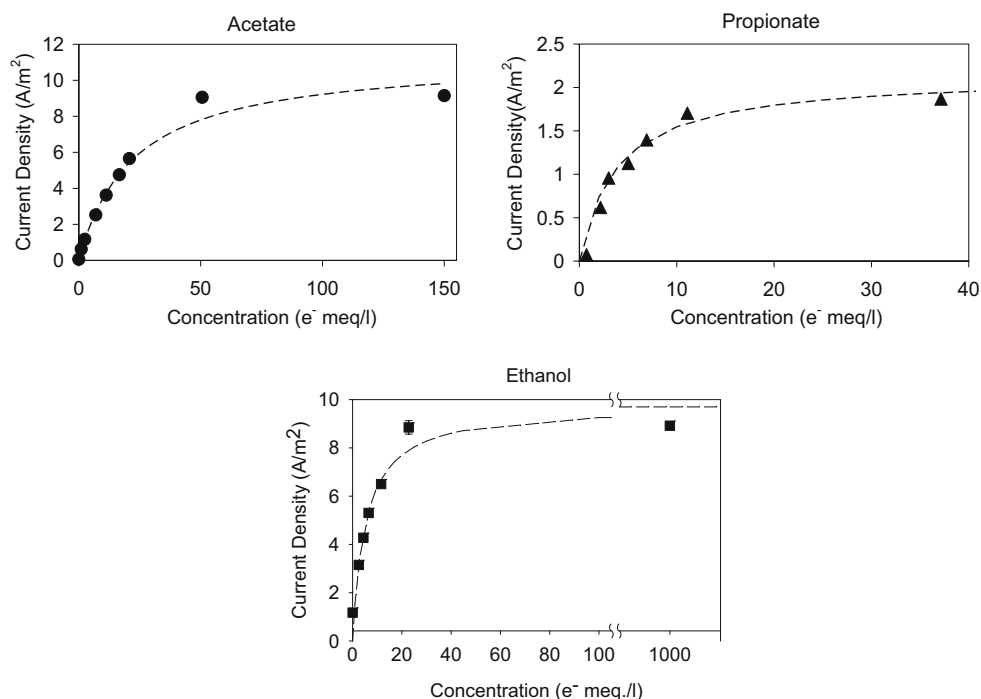


**Fig. 3** Concentration effect on current density for acetate, propionate, and ethanol as individual substrates at  $V_{\text{anode}}=0.1$  V vs Ag/AgCl. Dotted lines are Monod equation plots using parameters calculated from the data

much higher than for decay,  $\text{H}_2$ , and butyrate. Propionate showed a distinct saturation effect at about  $-0.3$  V. Based on the current densities in Fig. 2, acetate and ethanol were the fermentation products that were consumed most effectively in the MEC. We also calculated coulombic efficiencies for acetate, ethanol, and propionate during the initial stabilization period for each substrate: They were 86, 49, and 41%, respectively.

We evaluated the effect of substrate concentration on current density by varying the concentration of acetate, propionate, and ethanol inside the reactor. Figure 3 shows the results, which have Monod-like saturation shapes. We estimated the best-fit half-saturation constants ( $K_{s, \text{app}}$ ) and maximum current density ( $j_{\text{max}}$ ) using the relative least-squares method (Sáez and Rittmann 1992).  $K_{s, \text{app}}$  for acetate, ethanol, and propionate were 22, 5.3, and 3.8  $e^-$  meq/l (2.8, 0.44, and 0.27 mM), respectively. These  $K_{s, \text{app}}$  values for acetate and ethanol are consistent with previous results in an MFC (19  $e^-$  meq/l from acetate by Liu et al. 2005b; 0.18–58  $e^-$  meq/l for ethanol by Kim et al. 2007). The  $K_{s, \text{app}}$  value for propionate is reported here for the first time.

## Discussion

### Butyrate and hydrogen consumption by ARB

We obtained a low current density from butyrate in our continuous experiments (Fig. 2). Liu et al. (2005b)

measured current density from butyrate in a batch MFC, obtaining a significant current density ( $0.77 \text{ A/m}^2$ ), although it was about three times smaller than that obtained in their experiments with acetate. In their butyrate experiments, a considerable amount of acetate was present in the reactor, indicating the possibility that butyrate was fermented to acetate, which was consumed by the ARB. Given

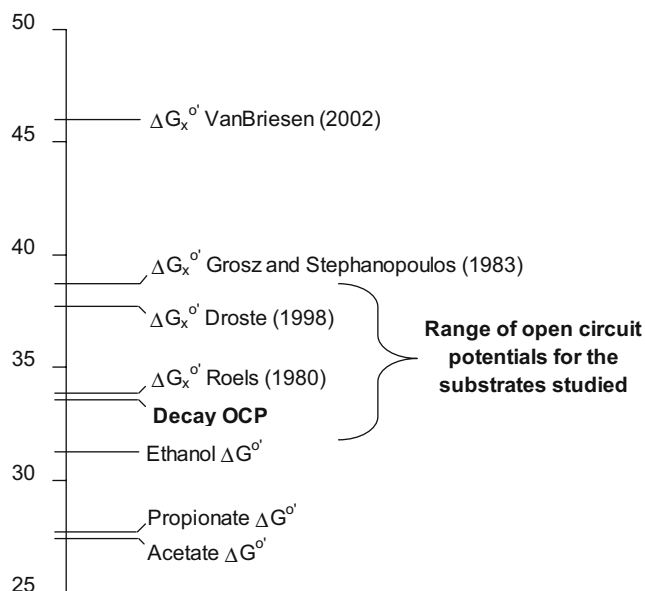


**Fig. 4** Gibbs free energy scale ( $\text{kJ}/e^- \text{ eq}$ ) for the substrates and fermentation products of interest, the measured OCPs, and estimated standard free energy for biomass from the literature

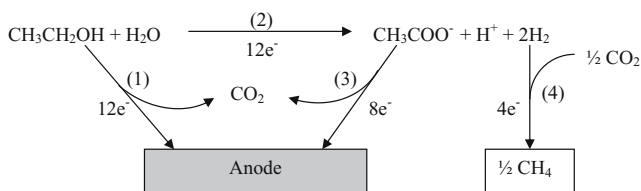


**Fig. 5** Schematic of possible reactions occurring during ethanol consumption. 1 Ethanol is consumed by ARB, and electrons are transferred to the electrode. 2 Ethanol is fermented to acetate and  $\text{H}_2$  by fermenters. 3 Acetate produced during fermentation is consumed by ARB. 4 Given that our ARB community cannot consume  $\text{H}_2$  and that  $\text{H}_2$  was not measured in our reactors, methanogens consume the  $\text{H}_2$  produced during fermentation, making  $\text{CH}_4$  an  $e^-$  sink

that the energy available for butyrate fermentation to acetate is very small ( $\sim 3$  mV at standard conditions), we hypothesize that, due to our continuous operation, bacteria capable of fermenting butyrate were washed out of our system, leading to a smaller current density compared to the other organic substrates.

$\text{H}_2$  also was not effectively consumed in our MEC experiments (Fig. 2); similar results were also reported by Lee et al. (2003). In contrast, Bond and Lovley (2003) produced a current with  $\text{H}_2$  similar to that obtained with acetate using a pure culture of *Geobacter sulfurreducens*. Although their experiments were conducted only for a few hours, their results are the only indication that rapid consumption of  $\text{H}_2$  by ARB is possible. An ARB community that is unable to consume  $\text{H}_2$  effectively can lead to a decrease in coulombic efficiency if fermentation and MEC are combined in one reactor when the  $\text{H}_2$  is consumed to form  $\text{CH}_4$  or escapes without oxidation.

### Open-cell potential

The anode voltage that occurs for zero current is called the OCP, and it indicates the equilibrium thermodynamic potential of the reaction with the electrode. Decay showed an OCP of  $-0.54$  V vs Ag/AgCl (Fig. 2a). This OCP

converts to  $33.3 \text{ kJ/e}^- \text{ eq}$  (Ag/AgCl is  $+0.197$  V with respect to SHE). The use of an MEC/MFC to measure OCP for decay gives, for the first time, a direct experimental value that is related to the thermodynamic free energy half-reaction of biomass components that undergo endogenous oxidation. Various researchers calculated, directly or indirectly, the free energy half-reaction of biomass ( $\Delta G_X^{\circ'}$ ) based on empirical data and model estimations and aimed to correlate thermodynamics with bacterial yields (Roels 1980; Grosz and Stephanopoulos 1983; Droste 1998; VanBriesen 2002). Other researchers have assumed that  $\Delta G_X^{\circ'}$  is similar to the free energy of oxidation of the electron donor used (Heijnen et al. 1992); this concept, called energetic regularity, was used to simplify model development. Figure 4 plots our biomass free energy (labeled Decay OCP) together with previous estimates. Our value of  $33.3 \text{ kJ/e}^- \text{ eq}$  is similar to the estimate by Roels (1980) for biomass free energy ( $33.8 \text{ kJ/e}^- \text{ eq}$ ), but lower than most other estimated values:  $38.6 \text{ kJ/e}^- \text{ eq}$  by Grosz and Stephanopoulos (1983),  $37.7 \text{ kJ/e}^- \text{ eq}$  by Droste (1998), and  $46.0 \text{ kJ/e}^- \text{ eq}$  by VanBriesen (2002). Our value could be lower than these values because respiration by the ARB is directly connected to the oxidation of simple intercellular molecules that are produced from the hydrolysis of the complex cell components that must be synthesized to produce cell walls, membrane, proteins, DNA, and RNA. Our value gives insight on the energy that bacteria can obtain from endogenous respiration.

Similarly, we measured the OCP of the MEC when fed with acetate, propionate, and ethanol (Fig. 2b). The range of OCPs we measured for the substrates are shown as free energy by the bracket in Fig. 4 ( $31.8$  to  $38.7 \text{ kJ/e}^- \text{ eq}$ ). The free energies of the OCPs for these substrates are higher than their respective  $\Delta G^{\circ'}$  values for the half reactions in Table 1, and they are closer to the OCP for biomass decay. Thus, the measured OCPs probably reflect the potential of simple molecules inside the cells (similar to endogenous respiration) not the exogenous substrate actually utilized.

**Table 2** Parameters obtained for the consumption of fermentation products in a continuous MEC at pH=7.4 and 30°C

Substrate	Observed maximum current density, $j_{\max}$ [ $\text{A/m}^2$ ]	Calculated maximum current density, $j_{\max}$ [ $\text{A/m}^2$ ]	Calculated substrate half saturation constant, $K_{s, \text{app}}$ [ $e^- \text{ meq/l}$ ]	Anode overpotential at $0.5 j_{\max}$ [V]	Coulombic efficiency [%]
Acetate	9.0	11	22	0.32	86
Ethanol	8.2	9.7	5.3	0.25	49
Propionate	1.6	2.1	3.8	0.13	41
Butyrate	0.16				
$\text{H}_2$	0.13				
No substrate	0.07				
			No experiments performed		

Monod  $j_{\max}$  and  $K_{s, \text{app}}$  were estimated by a relative least-squares method. The anode overpotential reported is the potential loss (vs OCP) required to achieve one half of  $j_{\max}$

## Coulombic efficiency

Clearly, acetate had the highest coulombic efficiency, and the difference probably is related to the fact that ethanol and propionate can be fermented to acetate and H<sub>2</sub>. During the ethanol experiment, we recorded acetate concentrations of 4 to 7 e<sup>-</sup> meq/l, documenting that ethanol fermentation occurred; this occurrence was also reported by Kim et al. (2007) in an ethanol MFC. Besides acetate, ethanol is fermented to 2 mol of H<sub>2</sub> (Metje and Frenzel 2005); this is a diversion of 33% of the electrons to H<sub>2</sub>, which was not effectively converted to electrical current.

Figure 5 illustrates how acetate and H<sub>2</sub> can compete as electron sinks with direct anode respiration. Given that our ARB community was not able to consume H<sub>2</sub> effectively, H<sub>2</sub> produced by ethanol fermentation was lost from the electron flow to the anode and probably ended up in CH<sub>4</sub> (Fig. 5). We measured headspace CH<sub>4</sub> and H<sub>2</sub> for ethanol and mixed-substrates experiments. The ethanol experiment showed 26% methane in the reactor headspace and negligible H<sub>2</sub> vs 3.4% methane when a mixture of substrates was fed into the MEC. Thus, CH<sub>4</sub> appeared to be an important electron sink for ethanol.

Unlike H<sub>2</sub>, acetate produced during ethanol fermentation can be consumed efficiently by ARB, resulting in current generation. Based on the results we have, we cannot determine what fraction of the electrons circuit were produced through acetate as intermediate vs direct ethanol consumption by ARB. However, the acetate concentration increased up to 26 e<sup>-</sup> meq/l during a period of 10 h with open-circuit conditions, indicating that acetate was produced during fermentation and then consumed by ARB when the circuit was closed. CH<sub>4</sub> and H<sub>2</sub> could also explain the low coulombic efficiency during the propionate experiment, although acetate was not present in recordable amounts. The conversion of propionate to acetate and H<sub>2</sub> as a first step of current generation in an MFC was already proposed by Oh and Logan (2005).

## Kinetic parameters

Table 2 shows a summary of the parameters we obtained for the various fermentation products. These parameters are important for the design and feasibility analysis of an MFC/MEC system that is fed a fermentation effluent. Acetate showed the highest current density and coulombic efficiency, but a higher anode overpotential and  $K_{s, app}$ . On the other hand, ethanol showed a high current density, smaller anode overpotential, and lower  $K_{s, app}$ , but with a lower coulombic efficiency due to methanogenesis. Propionate was consumed at lower current densities, but it is still a feasible fermentation product for MFC/MEC current generation if produced at low concentrations. Although

butyrate was not consumed at a considerable rate in our study, previous batch studies show its feasibility as a substrate; this finding suggests that butyrate consumption by ARB might require a longer retention time to maintain all bacteria involved in its oxidation. Given these results, we conclude that acetate/ethanol type fermentation (Ren et al. 1997) would be the best pretreatment for the ARB community developed in our reactor.

Methane production apparently was a significant e<sup>-</sup> sink during the ethanol experiments. From our results, it is evident that ARB have a lower  $K_S$  value for acetate than methanogens (~7 mM; Kus and Wiesmann 1995; Rittmann and McCarty 2001). However, H<sub>2</sub> produced, if any, could be converted to methane due to the inability of our ARB community to consume it. Thus, the competition between ARB and methanogens for nutrients and substrate should be studied in more detail to search for conditions at which methanogens are outcompeted.

**Acknowledgment** The funding for this work was provided by OpenCEL and NZ Legacy.

## References

- Bard AJ, Faulkner LR (2001) Electrochemical methods. Wiley, New York
- Bond DR, Lovley DR (2003) Electricity production by *Geobacter sulfurreducens* attached to electrodes. Appl Environ Microb 69:1548–1555
- Chaudhuri SK, Lovley DR (2003) Electricity generation by direct oxidation of glucose in mediatorless microbial fuel cells. Nat Biotechnol 21:1229–1232
- Dentel SK, Strogen B, Chiu P (2004) Direct generation of electricity from sludges and other liquid wastes. Water Sci Technol 50:161–168
- Droste RL (1998) Endogenous decay and bioenergetics theory for aerobic wastewater treatment. Water Res 32:410–418
- Grosz R, Stephanopoulos G (1983) Statistical mechanical estimation of the free-energy of formation of *E. coli* biomass for use with macroscopic reactor balances. Biotechnol Bioeng 25:2149–2163
- Heijnen JJ, van Loosdrecht MCM, Tjihuis L (1992) A black box mathematical model to calculate auto- and heterotrophic biomass yields based on Gibbs energy dissipation. Biotechnol Bioeng 40:1139–1154
- Hwang MH, Jang NJ, Hyun SH, Kim IS (2004) Anaerobic bio-hydrogen production from ethanol fermentation: the role of pH. J Biotechnol 111:297–309
- Kato Marcus A, Torres CI, Rittmann BE (2007) Conduction based modeling of the biofilm anode of a microbial fuel cell. Biotechnol Bioeng (in press). DOI 10.1002/bit.21533
- Kim JR, Jung SH, Regan JM, Logan BE (2007) Electricity generation and microbial community analysis of alcohol powered microbial fuel cells. Bioresour Technol 98:2568–2577
- Kus F, Wiesmann U (1995) Degradation kinetics of acetate and propionate by immobilized anaerobic mixed cultures. Water Res 29:1437–1443
- Lee JY, Phung NT, Chang IS, Kim BH, Sung HC (2003) Use of acetate for enrichment of electrochemically active microorganisms and their 16S rDNA analyses. FEMS Microbiol Lett 223:185–191

- Liu H, Grot S, Logan BE (2005a) Electrochemically assisted microbial production of hydrogen from acetate. *Environ Sci Technol* 39:4317–4320
- Liu H, Cheng SA, Logan BE (2005b) Production of electricity from acetate or butyrate using a single-chamber microbial fuel cell. *Environ Sci Technol* 39:658–662
- Metje M, Frenzel P (2005) Effect of temperature on anaerobic ethanol oxidation and methanogenesis in acidic peat from a northern wetland. *Appl Environ Microb* 71:8191–8200
- Min B, Logan BE (2004) Continuous electricity generation from domestic wastewater and organic substrates in a flat plate microbial fuel cell. *Environ Sci Technol* 38:5809–5814
- Min B, Kim JR, Oh SE, Regan JM, Logan BE (2005) Electricity generation from swine wastewater using microbial fuel cells. *Water Res* 39:4961–4968
- Oh SE, Logan BE (2005) Hydrogen and electricity production from a food processing wastewater using fermentation and microbial fuel cell technologies. *Water Res* 39:4673–4682
- Picioreanu C, Heam IM, Katuri KP, van Loosdrecht MCM, Scott K (2007) A computational model for biofilm-based microbial fuel cells. *Water Res* 41:2921–2940
- Rabaey K, Verstraete W (2005) Microbial fuel cells: novel biotechnology for energy generation. *Trends Biotechnol* 23:291–298
- Rabaey K, Van de Sompel K, Maignien L, Boon N, Aelterman P, Clauwaert P, De Schamphelaire L, Pham HT, Vermeulen J, Verhaege M, Lens P, Verstraete W (2006) Microbial fuel cells for sulfide removal. *Environ Sci Technol* 40:5218–5224
- Sáez PB, Rittmann BE (1992) Model-parameter estimation using least-squares. *Water Res* 26:789–796
- Ren NQ, Wang BZ, Huang JC (1997) Ethanol-type fermentation from carbohydrate in high rate acidogenic reactor. *Biotechnol and Bioeng* 54:428–433
- Rittmann BE, McCarty PL (2001) *Environmental biotechnology: principles and applications*. McGraw-Hill, New York, USA
- Roels JA (1980) Application of macroscopic principles to microbial metabolism. *Biotechnol Bioeng* 22:2457–2514
- VanBriesen JM (2002) Evaluation of methods to predict bacterial yield using thermodynamics. *Biodegradation* 13:171–190
- Wang J (2000) *Analytical Electrochemistry*. Wiley, Chichester, England
- Wu JH, Lin CY (2004) Biohydrogen production by mesophilic fermentation of food wastewater. *Water Sci Technol* 49:223–228
- Ying Z, Yang ST (2004) Effect of pH on metabolic pathway shift in fermentation of xylose by *Clostridium tyrobutyricum*. *J Biotechnol* 110:143–157
- Yu HQ, Fang HHP (2003) Acidogenesis of gelatin-rich wastewater in an upflow anaerobic reactor: influence of pH and temperature. *Water Res* 37:55–66
- Zhang XC, Halme A (1995) Modeling of a microbial fuel-cell process. *Biotechnol Lett* 17:809–814